

Discovery of mafic impact melt in the center of the Vredefort Dome; archetype for continental residua of Early Earth cratering?

C. L. Cupelli^{1*}, D.E. Moser¹, I.R. Barker¹, J.R. Darling², J.R. Bowman³, and B. Dhuime^{4,1}

Earth Science, Western University, 1151 Richmond Street, London, Ontario N6A 5B7, Canada.

²*University of Portsmouth, Burnaby Building, Burnaby Road, Portsmouth P01 3QL, UK*

³*Geology and Geophysics, University of Utah, 115 S 1460E, Salt Lake City, Utah 84112, USA.*

⁴*Earth Sciences, University of Bristol, Wills Memorial Building, Queens Road, Bristol BS8 1RJ, UK.*

ABSTRACT

Melting by impact heating is thought to have been a significant process in the modification of early planetary crusts, however, apart from the Sudbury and Manicouagan melt sheets, crustally derived melt bodies in ancient terrestrial crust are frequently presumed absent due to erosion. Here we demonstrate in the central basement uplift of the 2.020 Ga Vredefort impact basin that components of mafic impact melt have survived amidst Archean gneiss as dm-scale dykes and lenses of variably foliated gabbro-norite. Zircon microstructural, trace element and isotopic analysis (U-Pb, Lu-Hf) of the gabbro-norite reveals a dominant population of 2.02 Ga unshocked igneous zircon with apparent Ti-in zircon temperatures of 800–900°C, similar to those from the mafic Sublayer of the Sudbury impact melt sheet. Highly negative, subchondritic ϵ_{Hf} values of -1.4 ± 1.1 to -7.9 ± 1.4 are consistent with a depleted mantle model age of ~3 Ga and gabbro-norite derivation from the once superjacent Witwatersrand basin lithologies. The recrystallized igneous mineral textures and Archean felsic gneiss inclusions in the gabbro-norite

are attributable to the effects of emplacement and crater modification following ~20 km elevation of the central uplift. Long mistaken as pre-impact basement, the setting and characteristics of the Vredefort gabbro-norite may provide new benchmarks in the search for remnants of large cratering events and melt residua on Earth's cratons.

INTRODUCTION

Large-scale impact heating and melting of crust is thought to have been important on the Early Earth (Kring and Cohen, 2002), yet interactions at melt-lithosphere contacts in the central uplift of large craters are rarely exposed in terrestrial targets and remain poorly understood (Grieve and Cintala, 1992; Wielicki et al., 2012). The question is; what do the deep levels of large, deeply eroded impact structures look like (Garde et al., 2012)? The 2.020 Ga Vredefort impact structure of South Africa (Spray et al., 1995; Kamo et al., 1996; Moser, 1997) is an ideal site to address such questions. It is among the largest of the known terrestrial impact structures, with a rim-to-rim diameter of the collapsed transient cavity of ~160 km (Bishopp, 1962), and the structure extends vertically ~20 km into the Mesoarchean Kaapvaal craton (Henkel and Reimold, 1998). The Vredefort crater, like Sudbury, would have been filled by an extensive melt sheet several kilometers thick derived from the Archean and Proterozoic target rocks (Ivanov, 2005). However, only three impact-related igneous units have so far been widely accepted: pseudotachyllite dykes and allochthonous radially distributed granophyre dykes (Walraven et al., 1990; Kamo et al., 1996) that intrude the outer Archean crystalline bedrock of the central uplift, and an autochthonous dm-scale granitic body at the center of the uplift, referred to as the Central Anatectic Granite, dated at 2017 ± 5 Ma (Gibson et al., 1997) and considered to be a partial melt of a ~300 km² area of recrystallized felsic Archean gneiss, the Inlandsee Leucogranofels (ILG). No vestiges of the impact melt sheet have been recognized with the possible exception of a 0.5 m

wide, foliated mafic dyke with a zircon age of 2019 ± 2 Ma (Moser, 1997). Other works have since proposed that this unit is instead a recrystallized mafic pseudotachyllite, due to the presence of inclusions of Archean felsic gneiss (ILG) in drill core (Gibson, and Reimold, 2008), and that its impact-age zircons are the result of post impact metamorphism (Gibson et al., 1998). We present regional and detailed mapping in a ~ 2 km² area of ILG bedrock in the vicinity of the foliated mafic dyke near the center of the Vredefort structure that reveals additional, larger occurrences of the mafic unit, and test for its impact origin with detailed mapping of contact relationships and analyses of zircon U-Pb and Lu-Hf isotopic composition, microstructure and Ti abundance for the purpose of thermometry.

METHODS

Bedrock exposure in the central uplift region (Fig. 1) is very low (<1%) and reconnaissance mapping of a 2 km² area north of the Inlandsee Pan revealed two areas of outcrop of mafic rock similar to the ‘type’ mafic dyke (Moser, 1997). Sites (1 and 2) were subsequently mapped at a 10 m grid spacing to define the contact relationships and extent of the mafic bodies prior to sampling. Zircon analytical methods are given in detail in Supplementary Material.

RESULTS

Field Relationships and Mineral Textures

The bedrock at Sites 1 and 2 consists of polydeformed Archean ILG (granodioritic gneiss) with minor meta-ironstone inclusions, as is typical of the region (Stephens, 1990). We report that within this are lenticular to dyke-like bodies of mafic composition that exhibit rubbly, spheroidal weathering surfaces and sharp contacts with the Mesoarchean granitoid gneiss (Fig. 2). The map pattern is either a bifurcating or stockwork distribution, or trains of amoeboid-shaped bodies. Variations of mineral abundances determined using energy dispersive

spectroscopy (EDS) analysis place the rock type at the boundary of gabbroic and noritic classification fields, and for simplicity is referred to here as gabbronorite. The pyroxenes have inverted pigeonite exsolution lamellae and subhedral to anhedral grain boundaries indicate some recrystallization. Similar textures were described for units interpreted as Archean mafic granulite by early workers (Schreyer et al., 1978; Stepto, 1990). Gabbronorite bodies display a range of mineral textures from medium-grained and massive to weakly foliated at the center, to strongly foliated and finer grained near contacts with ILG. The fabric is defined by alignment of mafic and oxide minerals (Fig. DR1 in the GSA Data Repository) but no evidence of shock microstructures or metamorphism was observed in the rock-forming minerals of the gabbronorite at either site.

Zircon microstructure, thermometry and U-Pb Geochronology

Zircon imaging (cathodoluminescence (CL) and backscatter electron (BSE)), geochronology (U-Pb), and Ti thermometry were performed on zircon separates from samples of the 'type' mafic dyke at Site 1 (V250), and two samples from Site 2. The Site 2 samples are of a fine grained (V235) and coarse grained (V232) massive gabbronorite. Lu-Hf analysis was also performed on zircons from samples V250 and V235. The CL reveals dominantly unshocked euhedral to subhedral grains with sharp oscillatory concentric planar growth bands (Fig. DR2 in the GSA Data Repository) typical of igneous zircon (Corfu et al., 2003); likewise the co-existing baddeleyite is euhedral and shows no evidence of shock (Moser et al., 2013). Mapping and imaging of zircon type and location in thin section (Fig. DR1) reveals a random distribution relative to mineralogy, consistent with an igneous paragenesis. This is in sharp contrast with the neighboring ILG gneiss in which CL and EBSD analysis shows that zircons contain shock features such as microtwins over-printed by post-shock recrystallization (Fig. 2C) (Moser et al.,

2011). A subpopulation of gabbro-norite zircons exhibits irregular to chaotic CL patterns, planar features, and a higher abundance of inclusions similar to ILG zircons and these are interpreted as xenocrysts from the host felsic gneiss (Fig. 2B) (Moser, 1997; Moser et al., 2011). Based on thin section analysis, xenocrysts are slightly more abundant (~60%) than igneous grains in the narrow gabbro-norite dyke from Site 1 suggesting significant crustal contamination, whereas in samples V232 and V235 of the larger body at Site 2, igneous grains are dominant (>90%). SHRIMP U-Pb data from the igneous zircons are generally concordant, with evidence of weak discordance due to a minor 1.1 Ga Pb-loss event known in the region (Moser et al. 2011). The upper intercept age for igneous zircons from V250 is 2036 ± 45 Ma, in agreement with the ID-TIMS age of 2019 ± 2 Ma for this sample (Moser, 1997). Data for igneous zircons from samples V232 and V235 have a combined upper intercept age of 2039 ± 33 Ma, also overlapping the 2020 ± 3 Ma age of impact.

Ti-in-zircon thermometry of igneous zircons from V250, V232 and V235, was calculated using a TiO_2 activity = 0.7 due to the presence of ilmenite in all the samples (Ghent and Stout, 1984; Ferry and Watson, 2007). The apparent (Fu et al., 2008) Ti-in-zircon crystallization temperatures range from $928 \pm 10^\circ\text{C}$ to $795 \pm 8.7^\circ\text{C}$. One grain from V235 shows core to rim apparent temperature decrease of $\sim 40^\circ\text{C}$ and three zircons from sample V232 show an average core to rim decrease of $\sim 50^\circ\text{C}$.

Lu-Hf Isotope Composition

Six igneous grains and two xenocrysts from sample V250 (Site 1) and eight igneous grains from sample V235 (Site 2) were analysed. The igneous grains from Site 1 have ϵ_{Hf} of -1.4 to -5.3 , and the grains from Site 2 have ϵ_{Hf} of -5.4 to -7.9 (Fig. 3). The two xenocrysts from V250 were not analyzed for U-Pb age, but are assumed to have had a primary age between

2.7 and 3.2 Ga based on xenocryst dating in this unit (Moser, 1997; Moser et al., 2011). When modeled at these ages, the xenocryst ϵ_{Hf} values are +0.4 and +11, respectively. The depleted mantle age of the source of the gabbro-norite magma is also between 2.7 Ga and 3.2 Ga assuming a $^{176}\text{Lu}/^{177}\text{Hf}$ reservoir value of 0.021 for crust derived from melting of mafic crust (Kemp et al., 2006).

DISCUSSION

Our new mapping, petrologic, and zircon geochronology and geochemistry data reveal properties of the Vredefort gabbro-norite bodies that are consistent with an origin through impact melting of the Kaapvaal craton, with implications for ancient crustal and mineral residua (e.g. Cavosie et al., 2010). Pyroxene exsolution textures are typical of rapidly cooled gabbroic bodies and they show no evidence of shock metamorphism. The cogenetic spatial relationship of igneous-zoned zircon and coexisting baddeleyite with primary minerals, and the consistency of their ages with the previous ID-TIMS U-Pb zircon age of 2019 ± 2 Ma for this rock type (Moser, 1997), indicate crystallization shortly after the Vredefort impact event. An intrusive process is supported by the presence of ILG inclusions and the map pattern of the gabbro-norite, which is reminiscent of basal melt sheet embayments on the original crater floor at Sudbury (Morrison, 1984). The temperature range for the crystallization of Vredefort impact melt zircons is between 795–928°C, high for tectonically generated crustal melts (Wei et al., 2008) but in concordance with Ti-in-zircon temperatures of mafic basal units of the Sudbury Igneous Complex (Darling et al., 2009) and zircon saturation modeling (Wielicki et al., 2012). At the lower end of the temperature range our values overlap those of 750–810°C unshocked zircon from “mafic pseudotachylite breccias” (Wielicki et al., 2012) that are more likely a xenolithic transitional contact to gabbro-norite. Zircons from the ILG gneiss, however, are distinctively shocked and

partially recrystallized with disturbed Archean U-Pb ages (Moser 1997, Moser et al., 2011).

Similar microstructures are observed in SEM analysis of the 5-10 cm long felsic inclusions in the transition zone at Site 2, most simply interpreted as incomplete assimilation of ILG country rock into rapidly emplaced mafic melt.

The locally developed grain fabric within the gabbronorite bodies is the basis for their longstanding interpretation as pre-impact Archean rocks, however, the geochronology data dictate that this is a post-impact fabric restricted to this unit and its contacts and hence we call on its genesis by either flow and/or localized deformation during the crater modification stage. Numerical modeling by Ivanov (2005) points to an original melt sheet volume for the Vredefort impact structure of $\sim 13,000 \text{ km}^3$ that took $\sim 10 \text{ Myr}$ to cool at the base, in the aftermath of $\sim 20 \text{ km}$ of central crater excavation and rebound (Henkel and Reimold, 1996). Localized downward intrusion and deformation during subsequent isostatic readjustment of the crater floor, while the deep melt sheet remained molten, could explain the gabbronorite field and textural characteristics. This would have occurred after intrusion of the granophyre dykes in the outer regions of the central uplift, thought to be similar to the Sudbury offset dykes that formed before melt sheet differentiation (Lightfoot and Farrow, 2002).

The highly negative ϵ_{Hf} values for igneous zircon from the gabbronorite (Fig. 3) indicate that it crystallized from either a crustally-contaminated mantle melt, or a melt derived from Archean crust and/or derivative sediments. The highest ϵ_{Hf} values, from Site 1, could be interpreted as reflecting impact triggered mafic magmatism, which would bring into question how deeply the impact affected the crust and underlying mantle beyond impact-triggered flow at the crust-mantle boundary (Moser et al., 2009). However, the Hf model (depleted mantle) age for the gabbronorite source, which falls between 3.16–2.68 Ga (Fig. 3), also overlaps the Hf model

age of zircons from the Witwatersrand supergroup (Zeh and Gerdes, 2012) and Ventersdorp and Transvaal units (Stevenson and Patchett, 1990) that would have melted to form the Vredefort melt sheet. As a similar 3.2 Ga Sm-Nd model age is exhibited by the 2.02 Ga bronzite granophyre dykes that have crustal and meteoritic composition (Koeberl et al., 1996), a melt sheet origin for the gabbronorite is favoured. Taken together, we hypothesize an origin for the gabbronorite by downward injection from a large overlying differentiated melt sheet, similar to those at the Sudbury and Manicouagan (O'Connell-Cooper and Spray, 2011) impact structures, at some point during the crater modification stage. The large variation in ϵ_{Hf} values of V250 and V235, is similar to that seen in Sm-Nd compositions of the Sudbury Sublayer (Prevec et al., 2000) and at this point are attributed to isotopic variation in local, upper crustal target lithology.

The archetypal Archean cratonic crust is composed of multiply deformed granitoid gneisses, containing subordinate supra-crustal and mafic meta-igneous units, which exhibit one or more generations of mineral fabric (Kusky and Polat, 1999). Our evidence demonstrates that a $\sim 300 \text{ km}^2$ crustal assemblage with similar macroscopic features can also be created through ancient impact processes, and mistaken as tectonic in origin. Zircon igneous and shock microstructures, high Ti-in zircon crystallization temperatures and perhaps highly negative ϵ_{Hf} values allow discrimination of relict impact-generated igneous units, or their residual zircon, and are a useful guide in the search for surviving continental residua of the large impacts that almost certainly affected the early crust of our planet.

CONCLUSIONS

Detailed field mapping and petrographic analysis, along with zircon microstructural, trace element and isotopic data, indicate an impact melting origin for gabbronorite bodies within the Archean gneisses of the Vredefort Dome or central uplift. We interpret these bodies to be relicts

of the Vredefort impact melt sheet, injected into the basement during crater modification. Long mistaken as part of the deep crustal Archean gneiss assemblage, the discovery of this impactite provides an opportunity to study the relationship of the deep melt sheet and dynamic central crater floor in a large impact environment that is rarely accessible but perhaps more common on Early Earth continental crust. One may ask: how many more such impact-generated assemblages exist in today's cratonic fragments? Further characterization of the petrogenesis and fabric development of the Vredefort gabbro-norite bodies is under way. Their recognition makes the central region of the Earth's largest known impact an analogue site that is uniquely important in understanding crustal modification by impact processes.

ACKNOWLEDGEMENTS

The authors wish to acknowledge support from NSERC-DG grant to DEM as well as a NSF grant EAR 0510280 to JRB and DEM. Dr. Rodger Hart is kindly acknowledged for discussions in the field. The manuscript benefited from constructive reviews from Prof. J. Spray and an anonymous reviewer.

REFERENCES CITED

- Bishopp, D.W., 1962, The Vredefort Ring: A further consideration: *Geology*, v. 70, p. 500-502.
- Cavosie, A.J., Quintero, R.R., Radovan, H.A., and Moser, D.E., 2010, A record of ancient cataclysm in modern sand: Shock microstructures in detrital minerals from the Vaal River, Vredefort Dome, South Africa: *GSA Bulletin*, v.122, p. 1968-1980, doi: 10.1130/B30187.1.
- Corfu, F., Hanchar, J.M., Hoskin, P.W.O., and Kinny, P., 2003, Atlas of Zircon Textures, *in* Hanchar, J.M., and Hoskin, P.W.O., eds., *Reviews in Mineralogy and Geochronology*, v. 53, p. 469–500.

- Darling, J., Storey, C., and Hawkesworth, C., 2009, Impact melt sheet zircons and their implications for the Hadean crust: *Geology*, v. 37, p. 927–930, doi:10.1130/G30251A.1.
- Ferry, J.M., and Watson, E.B., 2007, New thermodynamic models and revised calibrations for the Ti-in-zircon and Zr-in-rutile thermometers: *Contributions to Mineralogy and Petrology*, v. 154, p. 429–437, doi:10.1007/s00410-007-0201-0.
- Fu, B., Page, F.Z., Cavosie, A.J., Fournelle, J., Kita, N.T. Lackey, J.S., Wilde, S.A., and Valley, J.W., 2008, Ti-in-zircon thermometry : applications and limitations: *Contributions to Mineralogy and Petrology*, v. 156, p.197-215.
- Ghent, E.D., and Stout, M.Z., 1984, TiO₂ activity in metamorphosed pelitic and basic rocks: Principles and applications to metamorphism in southeastern Canadian Cordillera: *Contributions to Mineralogy and Petrology*, v. 86, p. 248–255, doi:10.1007/BF00373670.
- Gibson, R.L., Armstrong, R.A., and Reimold, W.U., 1997, The age and thermal evolution of the Vredefort impact structure: A single-grain U-Pb zircon study: *Geochimica et Cosmochimica Acta*, v. 61, p. 1531–1540, doi:10.1016/S0016-7037(97)00013-6.
- Gibson, R.L., Reimold, W.U., and Stevens, G., 1998, Thermal-metamorphic signature of an impact event in the Vredefort Dome, South Africa: *Geology*, v. 26, p. 787–790, doi:10.1130/0091-7613(1998)026<0787:TMSOAI>2.3.CO;2.
- Gibson, R.L., and Reimold, W.U., 2008, *Geology of the Vredefort impact structure, a guide to sites of interest*: Council of Geoscience, Memoir 97, Pretoria, 181 p.
- Garde, A.A., McDonald, I., Dyck, B., and Keulen, N., 2012, Searching for giant, ancient impact structures on Earth: The Mesoarchean Maniitsoq structure, West Greenland: *Earth and Planetary Science Letters*, v. 337–338, p. 197–210, doi:10.1016/j.epsl.2012.04.026.

- Grieve, R.A.F., and Cintala, M.J., 1992, An analysis of differential impact melt-crater scaling and implications for the terrestrial impact record: *Meteoritics*, v. 27, p. 526–538, doi:10.1111/j.1945-5100.1992.tb01074.x.
- Grieve, R.A.F., Coderre, J.M., Robertson, P.B. and Alexopoulos, J., 1990, Microscopic planar deformation features in quartz of the Vredefort structure: Anomalous but still suggestive of an impact origin: *Tectonophysics*, v. 171, p. 185-200, doi:10.1016/0040-1951(90)90098-S.
- Hart, R.J., Andreoli, M.A.G., Tredoux, M., and DeWit, M.J., 1990, Geochemistry across an exposed section of Archaean crust at Vredefort, South Africa: With implications for mid-crustal discontinuities: *Chemical Geology*, v. 82, p. 21–50, doi:10.1016/0009-2541(90)90072-F.
- Henkel, H., and Reimold, W.U., 1996, Geophysical modeling and reconstruction of the Vredefort Impact Structure, South Africa: *Meteoritics & Planetary Science*, v. 31, p. 59.
- Henkel, H., and Reimold, W.U., 1998, Integrated geophysical modelling of a giant, complex impact structure: Anatomy of the Vredefort Structure, South Africa: *Tectonophysics*, v. 287, p. 1–20, doi:10.1016/S0040-1951(98)80058-9.
- Ivanov, B.A., 2005, Modeling of the largest terrestrial meteoritecraters: *Solar System Research*, v. 39, p. 381–409, doi:10.1007/s11208-005-0051-0.
- Kamo, S.L., Reimold, W.U., Krogh, T.E., and Colliston, W.P., 1996, A 2.023 Ga age for the Vredefort impact event and a first report of shock metamorphosed zircons in pseudotachylitic breccias and granophyres: *Earth and Planetary Science Letters*, v. 144, p. 369–387, doi:10.1016/S0012-821X(96)00180-X.

- Kemp, A.I.S., Hawkesworth, C.J., Paterson, B.A., and Kinny, P.D., 2006, Episodic growth of the Gondwana supercontinent from hafnium and oxygen isotopes in zircon: *Nature*, v. 439, p. 580-583, doi:10.1038/nature04505.
- Koerberl, C., Reimold, W.U., and Shirey, S.B., 1996, Re-Os isotope and geochemical study of the Vredefort Granophyre: Clues to the origin of the Vredefort structure, South Africa: *Geology*, v. 24, p. 913–916, doi:10.1130/0091-7613(1996)024<0913:ROIAGS>2.3.CO;2.
- Kring, D.A., and Cohen, B.A., 2002, Cataclysmic bombardment throughout the inner solar system 3.9–4.0 Ga: *Journal of Geophysical Research*, v. 107, p. 4–6, doi:10.1029/2001JE001529.
- Kusky, T.M., and Polat, A., 1999, Growth of granite-greenstone terranes at convergent margins, and stabilization of Archean cratons: *Tectonophysics*, v. 305, p. 43–73, doi:10.1016/S0040-1951(99)00014-1.
- Lightfoot, P.C., and Farrow, C.E.G., 2002, Geology, Geochemistry, and Mineralogy of the Worthington Offset Dike: A Genetic Model for Offset Dike Mineralization in the Sudbury Igneous Complex: *Economic Geology*, v. 97, p. 1419-1446.
- Morrison, G.G., 1984, Morphology of the Sudbury Structure in relation to an Impact Origin, *in* Pye, E.G., Naldrett, A.J., and Giblin, P.E., eds., *The Geology and Ore Deposits of the Sudbury Structure*: Ontario Geological Survey, Special Volume 1, p.513–520.
- Moser, D.E., 1997, Dating the shock wave and thermal imprint of the giant Vredefort impact, South Africa: *Geology*, v. 25, p. 7–10, doi:10.1130/0091-7613(1997)025<0007:DTSWAT>2.3.CO;2.

- Moser, D.E., Davis, W.J., Reddy, S.M., Flemming, R.L., and Hart, R.J., 2009, Zircon U-Pb strain chronometry reveals deep impact-triggered flow: *Earth and Planetary Science Letters*, v. 277, p. 73–79, doi:10.1016/j.epsl.2008.09.036.
- Moser, D.E., Cupelli, C.L., Barker, I.R., Flowers, R.M., Bowman, J.R., Wooden, J., and Hart, J.R., 2011, New Zircon Shock Phenomenon and their use for Dating and Reconstruction of Large Impact Structures Revealed by Electron Nanobeam (EBSD, CL, EDS), and Isotopic U-Pb, and (U-Th)/He Analysis of the Vredefort dome: *Canadian Journal of Earth Sciences*, v. 4, p. 117–139.
- Moser, D.E., Chamberlain, K.R., Tait, K.T., Schmitt, A.K., Darling, J.R., Barker, I.R., and Hyde, B.C., 2013, Solving the Martian meteorite age conundrum using micro-baddeleyite and launch-generated zircon: *Nature*, v. 499, p. 454–457, doi:10.1038/nature12341.
- O'Connell-Cooper, C.D. and Spray, J.G., 2011, Geochemistry of the impact-generated melt sheet at Manicouagan: Evidence for fractional crystallization: *Journal of Geophysical Research (Solid Earth)*, v. 116, B06204, doi:10.1029/2010JB008084.
- Prevec, S.A., Lightfoot, P.C., and Keays, R.R., 2000, Evolution of the Sublayer of the Sudbury Igneous Complex: Geochemical, Sm-Nd isotopic and petrologic evidence: *Lithos*, v. 51, p. 271–292, doi:10.1016/S0024-4937(00)00005-0.
- Schreyer, W., Stepto, D., Abraham, K., and Muller, W.F., 1978, Clinoeulite (Magnesian Clinoferrosilite) in a Eulysite of a Metamorphosed Iron Formation in the Vredefort Structure, South Africa: *Contributions to Mineralogy and Petrology*, v. 65, p. 351–361, doi:10.1007/BF00372283.

- Spray, J.G., Kelley, S.P., and Reimold, W.U., 1995, Laser probe argon-40/argon-39 dating of coesite and stishovite-bearing pseudotachylytes and the age of the Vredefort impact event: *Meteoritics*, v. 30, p. 335–343, doi:10.1111/j.1945-5100.1995.tb01132.x.
- Stepro, D., 1990, The geology and gravity field in the central core of the Vredefort structure: *Tectonophysics*, v. 171, p. 75–103, doi:10.1016/0040-1951(90)90091-L.
- Stevenson, R.K., and Patchett, P.J., 1990, Implications for the evolution of continental crust from Hf isotope systematic of Archean detrital zircons: *Geochimica et Cosmochimica Acta*, v. 54, p. 1683–1697, doi:10.1016/0016-7037(90)90400-F.
- Walraven, F., Armstrong, R.A., and Kruger, F.J., 1990, A chronostratigraphic framework for the north-central Kaapvaal craton, the Bushveld Complex and the Vredefort structure: *Tectonophysics*, v. 171, p. 23–48, doi:10.1016/0040-1951(90)90088-P.
- Wei, C.S., Zhao, Z.F., and Spicuzza, M.J., 2008, Zircon oxygen isotopic constraint on the sources of late Mesozoic A-type granites in eastern China: *Chemical Geology*, v. 250, p. 1–15, doi:10.1016/j.chemgeo.2008.01.004.
- Wielicki, M.M., Harrison, T.M., and Schmitt, A.K., 2012, Geochemical signatures and magmatic stability of terrestrial impact produced zircon: *Earth and Planetary Science Letters*, v. 321–322, p. 20–31, doi:10.1016/j.epsl.2012.01.009.
- Zeh, A., and Gerdes, A., 2012, U-Pb and Hf isotope record of detrital zircons from gold-bearing sediments of the Pietersburg Greenstone Belt (South Africa)—Is there a common provenance with the Witwatersrand Basin: *Precambrian Research*, v. 204–205, p. 46–56, doi:10.1016/j.precamres.2012.02.013.

FIGURES

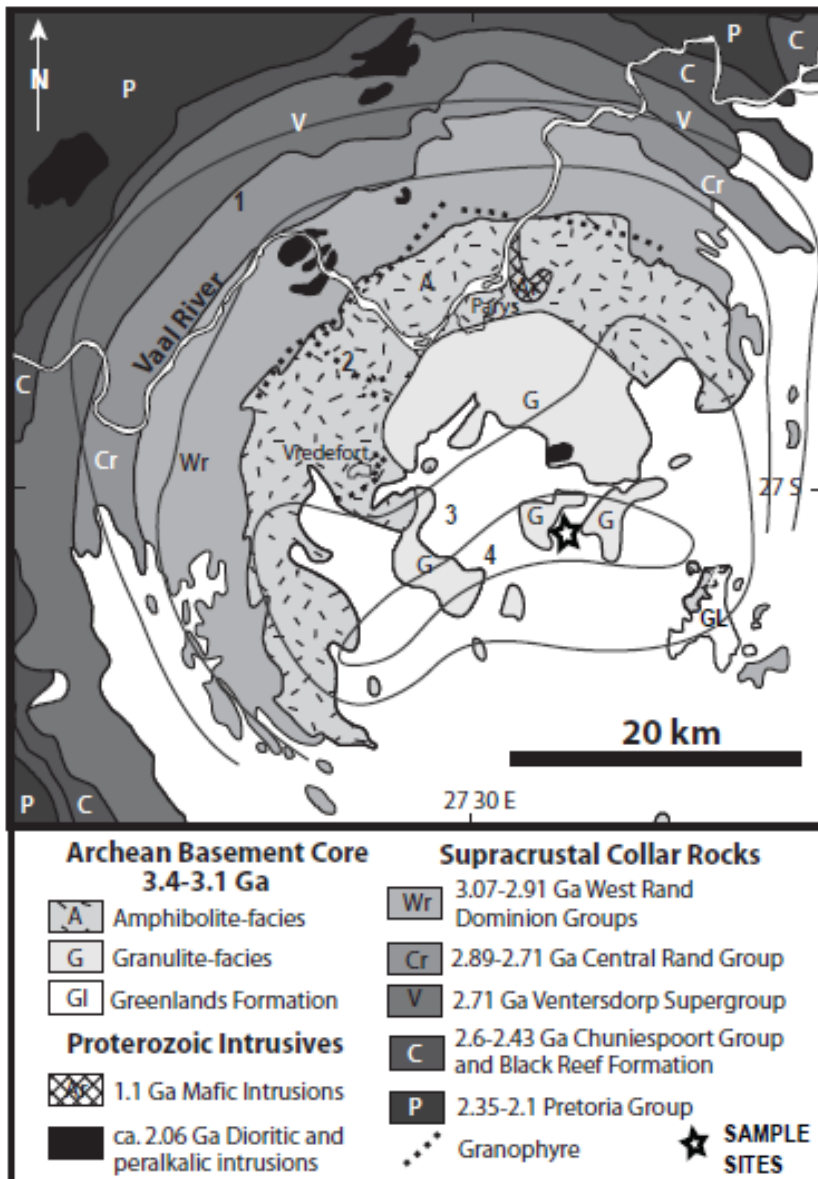


Figure 1. Generalized bedrock geology map of the Vredefort Dome (after Gibson and Reimold, 2008). Grey contours represent degree of post-shock thermal annealing of planar deformation features in quartz (Grieve et al., 1990), with zone 4 representing complete annealing and 1 representing the least annealing. Location of study area indicated with a star.

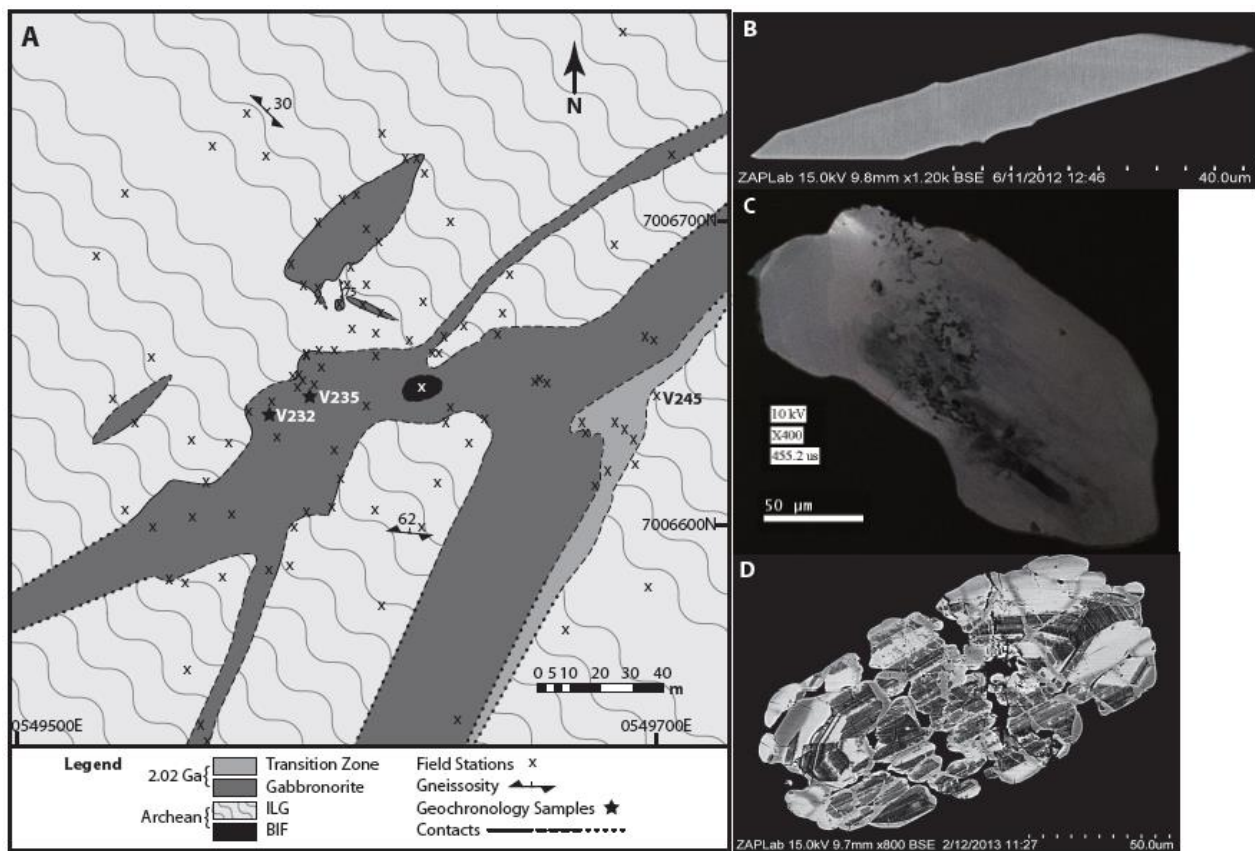


Figure 2. Geological map of Site 2 showing dykes and pods of gabbronorite within Mesoarchean ILG gneiss. The southeastern margin is referred to as the transition zone as it consists of a mixture of fine-grained gabbronorite and ILG units inter-fingered at the scale of meters to centimeters. Igneous zircon was analyzed from two Site 2 samples in the main body (A: V232 and B: V235). The BSE and CL images on the right show the typical zircon morphology for (A)

prismatic igneous zircon from gabbro-norite sample V235, (B) zircon with recrystallized xenocrystic core from gabbro-norite sample V232 (see also Moser et al., 2011) and (C) shocked recrystallized Archean zircon from ILG, proximal to the transition zone (location indicated by “C”).

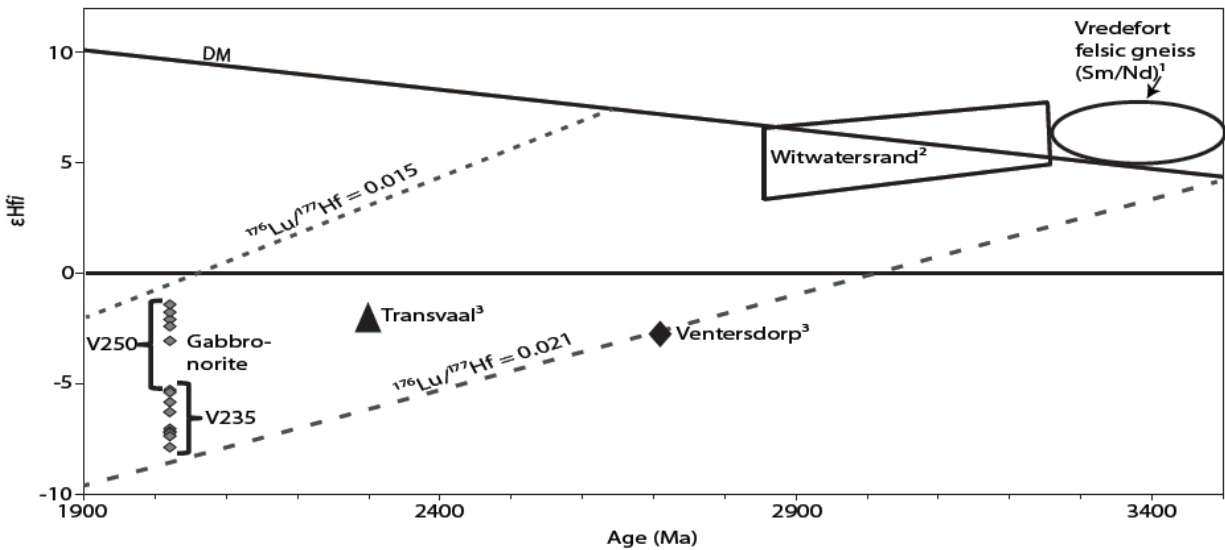


Figure 3. Plot of ϵ_{Hf} of gabbro-norite zircon at 2020 ± 3 Ma age of the impact compared to values for target lithologies. Samples from this study are shown as small gray diamonds. We use a Lu/Hf model ratio of 0.021 to determine the T_{DM} range of 3.2 to 2.7 Ga for the gabbro-norite source. The evolution path for the average continental crust with $^{176}\text{Lu}/^{177}\text{Hf} = 0.015$ is shown for comparison. The range of gabbro-norite T_{DM} overlaps the Sm/Nd model age for gneisses half way from the center of the Vredefort dome (oval, from Hart et al., 1990)¹; as well as zircon Hf T_{DM} for the Witwatersrand (box) (Zeh and Gerdes, 2012)², Ventersdorp (diamond) and Transvaal (triangle) (Stevenson and Patchett, 1990)³.